Ecohydrology

WILEY

RESEARCH ARTICLE OPEN ACCESS

Water Use Dynamics of Drought-Tolerant Coniferous Trees (*Pinus brutia* and *Cupressus sempervirens*) in a Semi-Arid Environment

Hakan Djuma[1] | Marinos Eliades[2] | Christos Zoumides[1] | Adriana Bruggeman[1]

[1]Energy, Environment and Water Research Center, The Cyprus Institute, Nicosia, Cyprus | [2]Environment and Climate Department, Eratosthenes Centre of Excellence, Limassol, Cyprus

Correspondence: Hakan Djuma (h.djuma@cyi.ac.cy)

Received: 10 February 2025 | **Revised:** 22 April 2025 | **Accepted:** 25 May 2025

Funding: This research has received financial support from the PRIMA (2018 Call) SWATCH Project and the Water JPI (Joint Call 2018) FLUXMED Project, both funded by the Republic of Cyprus through the Research and Innovation Foundation. The PRIMA programme is supported by Horizon 2020, the European Union's Framework Program for Research and Innovation. This study was also supported by Joint Programming Initiative Water Challenges for a Changing World and Partnership for Research and Innovation in the Mediterranean Area. This study was also supported by the REACT4MED (Inclusive Outscaling of Agro-Ecosystem Restoration Actions for the Mediterranean), funded by the PRIMA programme and supported by Horizon 2020 under Grant No. 2122.

Keywords: *Cupressus sempervirens* | drought tolerant trees | evapotranspiration | Mediterranean mixed forest | *Pinus brutia* | sap flow | soil water | water balance

ABSTRACT

Pinus brutia (pine) and *Cupressus sempervirens* (cypress) are two important forestry species in the Mediterranean region, with different strategies to cope with water stress. The overall goal of this study is to investigate ecohydrological processes of these two species. Specific objectives are (i) to quantify differences in sapflow of *P. brutia* and *C. sempervirens* trees during wet and dry seasons; (ii) to analyse effects of environmental variables on sapflow, leaf conductance (*gs*) and twig water potential (Ψ); and (iii) to analyse water balance components and soil water dynamics for three canopy cover conditions (under canopy, edge canopy and open area). The study site is a mixed forest in Cyprus, with an average annual rainfall of 315 mm. The site was planted in 2011 (average planting area: 30 m^2). Observations of sapflow (4 trees for 24 months and 8 trees for 20 months) and soil moisture (66 sensors, 24 months) were made hourly. Soil moisture sensors were installed in three canopy cover conditions, each at 10-, 30- and 50-cm soil depths. The sapflow over the canopy area of the trees during the November 2020 to June 2022 period was 642 mm for cypress and 314 mm for pine, under 581 mm rain. The partial correlation coefficient between daily sapflow and soil moisture was higher for pine than for cypress (0.66 vs. 0.31). Pine had a wider range of *gs* values and narrower range of Ψ values than cypress. Evapotranspiration from the open area was 14% higher than from under the tree canopy.

1 | Introduction

Climate scenarios predict an increase in the frequency and intensity of droughts during the growing season throughout Europe (IPCC 2023). The Mediterranean region will be one of the most affected areas as predictions show an increase in average temperatures and a reduction in precipitation in summer and spring for the coming decades (Zittis et al. 2022). Consequently, demand for afforestation has increased as trees store carbon and can potentially counterbalance the increasing CO_2 levels in the atmosphere (Chapman et al. 2020). In addition to storing carbon, trees have an important role in the water cycle (Ellison et al. 2017). Transpiration contributes a large share of terrestrial evapotranspiration (Jasechko et al. 2013;

Schlesinger and Jasechko 2014). The ecology and productivity of Mediterranean forests are particularly sensitive to climatic conditions (Scarascia-Mugnozza et al. 2000), and it remains a question if these forests will be able to adapt and survive in the upcoming decades (Vico et al. 2015).

The Mediterranean biome includes forests rich in conifers. The key to success of conifers in Mediterranean climate regions has been the evolution of functional hydraulic traits associated with drought tolerance, as exemplified by Neogene diversification in many clades of *Pinaceae* and *Cupressaceae* (Rundel 2019). *Pinus brutia* (*P. brutia*) and *Cupressus sempervirens* (*C. sempervirens*), two important forestry species in the Mediterranean region, are both established as natural forests and planted extensively in reforestation projects (Al-Hawija et al. 2014; Kostopoulou et al. 2010; Sevik and Cetin 2015). *P. brutia* is native to the eastern Mediterranean (mainly Turkey) and can be found as natural and naturalized stands from Greece to Azerbaijan and from the Black Sea coast of Georgia to the south of Israel. *C. sempervirens* is native to the eastern Mediterranean region and can be found from north of Tunisia and Libya and eastwards up to southeastern Iran (EUFORGEN 2025). In Turkey, natural *P. brutia* stands can occur in areas where annual average precipitation is between 400 and 2000 mm (Boydak 2004). *C. sempervirens* stands in Greece can occur in areas with annual average precipitation between 411 and 1452 mm (Brofas et al. 2006), although they can also grow in areas with 200 mm of annual rain (Caudullo and De Rigo 2016). Despite their widespread presence in water-limited regions, there are very few ecohydrological research articles on *P. brutia* (Houminer et al. 2022; Eliades et al. 2018) and *C. sempervirens* (Cohen et al. 2008; Lapidot et al. 2019; Rog et al. 2021; Schiller et al. 2004) in the Mediterranean region. Mixed tree species plantations have received attention from researchers as these were found to potentially reduce tree competition for water compared to single-species plantations (Bello et al. 2019; Magh et al. 2020; Rog et al. 2021). However, there is no research comparing *P. brutia* with *C. sempervirens* under the same environmental conditions.

Sap flow studies in Israel compared *C. sempervirens* with *Pinus halepensis* (*P. halepensis*) trees, a close relative of *P. brutia* with some morphological and physiological differences (Houminer et al. 2022). Cohen et al. (2008) summarized sap flow measurements from different climate regions of Israel. They reported that the range of sap velocities during noon, after significant rainfall, was two times higher for 15- and 19-year old *P. halepensis* trees in sub-humid and semi-arid regions than that of 15-year old *C. sempervirens* trees, for which no climatic region was specified. Rog et al. (2021) measured sap flow of 50-year-old *P. halepensis and C. sempervirens* trees, for 2–3 days every 2 months for a 2-year period in Yishi forest in Israel (average annual rainfall 510 mm). Contrary to Cohen et al. (2008), they found that average sap flux density ($g\,cm^{-1}\,day^{-1}$) of *P. halepensis* was lower than of *C. sempervirens* although they followed similar seasonal patterns. The above studies showed conflicting findings between sap velocities and sap flux densities of *C. sempervirens* and *P. halepensis* trees. Research on neighbouring *C. sempervirens* and *P. brutia* trees, with durations long enough to cover seasonal variations and with temporal resolutions fine enough to observe the effects of rainfall events and meteorological variables, could explain conflicting results and fill current research gaps.

Differences between *P. halepensis* and *C. sempervirens* have also been observed at leaf level (e.g., stomatal conductance and leaf water potential). Froux et al. (2005) subjected seedlings to soil drought in greenhouse experiments and found that seedlings of *P. halepensis* were more vulnerable to xylem embolism than those of *C. sempervirens*. In the open Yishi forest in Israel, in relatively wet conditions in March, Lapidot et al. (2019) observed lower leaf gas exchange rates and stomatal conductance of *P. halepensis*, compared with *C. sempervirens* trees. In contrast, Rog et al. (2021) observed higher stomatal conductance values for *P. halepensis* than *C. sempervirens* in the wet month of February in the same forest. Their predawn leaf water potential measurements at the end of dry season also indicated differences between *P. halepensis* and *C. sempervirens*. The above research showed that environmental variables have different effects on the regulation of leaf conductance and leaf water potential of *P. halepensis* and *C. sempervirens* species. However, these field studies were conducted in areas with an average annual rainfall around 500 mm, whereas these species have also been planted in drier environments.

One of the main uncertainties in estimating species-specific tree water use in semi-arid regions is the subsurface spatial heterogeneity of plant available water (Fan et al. 2017). Eliades et al. (2018) found from soil moisture observations and water balance computations that *P. brutia* trees on a steep mountain slope with shallow soil (average rainfall 425 mm $year^{-1}$) abstract water beyond the tree canopy area and from fractured bedrock, helping them survive dry summer months. However, their research was in a single-species forest with shallow soils (12-cm soil depth). Rog et al. (2021) analysed roots in soil samples and found that root growth of *C. sempervirens* is mostly horizontal and that of *P. halepensis* is both horizontal and vertical. Their modelling analysis showed that spatial differences in tree root zone water access can cause temporal differences in tree water use, especially in water-limited environments. However, they measured soil water content only in the centre of the forest plot. These studies showed differences in soil water use of *P. brutia*, *C. sempervirens* and *P. halepensis* species. However, they did not relate spatial variabilities in observed soil water content, as affected by tree canopy cover, to tree water use.

Linking internal tree hydraulics with soil water availability and water vapour exchange between tree and atmosphere in environments below an annual precipitation of 400 mm, which are considered beyond these trees' natural distribution (Boydak 2004), can provide important insights for afforestation strategies under a changing climate (e.g., species and spacing). The hypothesis of this research is that *P. brutia* and *C. sempervirens* trees have different water-use strategies, and these differences could be more pronounced in environments where rainfall is lower than in areas of their natural distribution. Therefore, the overall goal of this study is to investigate ecohydrological processes of two indigenous, drought-tolerant coniferous tree species with different physiological characteristic, that is, *P. brutia* and *C. sempervirens*, in a mixed plantation forest in a semi-arid environment. Specific objectives are (i) to quantify differences in sap flow of *P. brutia* and *C. sempervirens* trees during wet and dry seasons; (ii) to analyse effects of environmental variables (meteorological and soil water) on sap flow, leaf conductance and twig water potential of *P. brutia* and *C. sempervirens* trees; and (iii) to analyse

water balance components and soil water dynamics for three canopy cover conditions (under canopy, edge of canopy and open area) of *P. brutia* and *C. sempervirens* trees.

2 | Materials and Methods

2.1 | Study Site

The study site is located in Athalassa Forest Park, Cyprus (35°7′59.41″N, 33°24′1.77″E) and has a surface area of 10 ha with an average slope of 4%. Data from the Department of Meteorology station in Athalassa (< 1 km away) show a long-term average annual rainfall of 315 mm and an average temperature of 19.6°C (1980–2010). Average rainfall and temperature for the 1 November to 30 April wet period is 243 mm and 13.2°C, while for 1 May to 31 October it is 69 mm and 25.8°C. The mean daily minimum temperature is 5°C during January and February, and the mean daily maximum temperature is 37°C during July and August (1980–2010).

The site was converted from rain-fed agriculture to a mixed species forest by planting 2- and 3-year old seedlings of different, indigenous, drought-tolerant tree and shrub species, between November 2010 and February 2011. The ages of the trees and shrubs were 12 to 13 at the start of the 2-year monitoring period. In addition to *P. brutia* and *C. sempervirens* (henceforth referred as pine and cypress, respectively) (Figure 1), other main tree species are *Pistacia lentiscus*, *Pistacia atlantica*, *Olea europaea* and few individual trees of *Ceratona silique* and *Quercus coccifera*. The trees and shrubs are planted in rows and each plant is neighboured by six plants with 5 to 6 m distance between each other (Figure 2). The trees and shrubs were watered during the first 3 years after being planted. The seasonal vegetation between the trees is mowed each year in early summer.

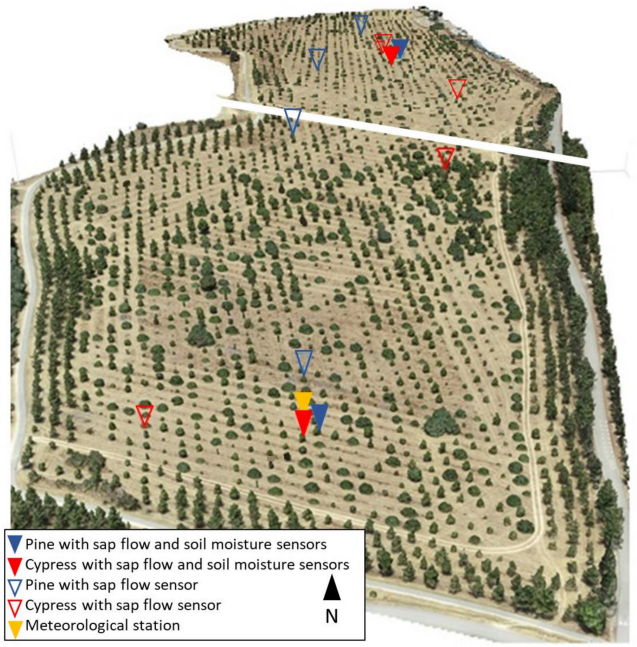

FIGURE 2 | 3D model of the study site and experimental layout, indicating the monitored trees and the meteorological station; north of the white line is the Athalassa formation, and south is the Nicosia formation (note that the image is tilted towards north, distances between trees are 5–6 m).

FIGURE 1 | *Pinus brutia* (a) and *C. sempervirens* (b) trees in Athalassa Forest Park study site.

The study site is located on two geological formations: Athalassa formation in the north and Nicosia formation in the south. Both are categorized as sedimentary formations. The Nicosia Formation was deposited during the Pliocene and contains grey and yellow siltstones and layers of calcarenites and marls and Athalassa formation was deposited later, during the early Pleistocene, and consists of calcarenites interlayered with sandy marls (Cyprus Geological Survey Department 1995).

Percussion drilling, at three random locations, showed soil depths of approximately 1 m. Soil samples for texture analyses were collected from 0–20 cm and 20–50 cm depths at four random locations (i.e., two on each geological formation). In one location on Athalassa formation, no soil sample could be collected from 20–50 cm depth due to presence of rocks. Texture of the 0–20 cm soil layer was sandy loam (59% sand, 28% silt and 13% clay) for one of the Nicosia formation locations and loamy sand (71%–80% sand, 20%–29% silt and 0% clay) for the other three locations. Texture of the 20–50 cm soil layer was sandy loam (62%–70% sand, 25%–30% silt and 0%–12% clay) at all three locations. Soil bulk density samples were collected at six random locations with 100-cm^3 rings from 0–10 cm and 40–50 cm soil depths. Average dry soil bulk density was 1.48 $g\,cm^{-3}$ (min: 1.33 $g\,cm^{-3}$, max: 1.60 $g\,cm^{-3}$) for the 0–10 cm depth and 1.54 $g\,cm^{-3}$ (min: 1.28 $g\,cm^{-3}$, max: 1.69 $g\,cm^{-3}$) for the 40–50 cm depth.

2.2 | Field Monitoring

2.2.1 | Field Surveys and Tree Mapping

The tree and shrub species were identified and mapped, and their stem diameter and characteristics (e.g., single or multiple stem) were recorded in February 2020. Table 1 presents the tree and shrub species names, number of plants and stem diameter of single stem plants on Athalassa and Nicosia geological formations. The stem diameter of plants with a single stem diameter larger than 8 cm was recorded to identify plants for possible sap flow sensor installation. A 3D digital surface model of the site with a horizontal and vertical resolution of 3 cm was constructed from areal images taken in June 2020 with an Unmanned Aerial Vehicle equipped with a DJI Phantom4 camera and a built-in Real Time Kinematic-Global Navigation Satellite System, based on the methodology of Obanawa et al. (2019) (Figure 2).

2.2.2 | Sap Flow Monitoring and Tree Biometrics

On each geological formation (Athalassa and Nicosia), four trees (two pine and two cypress) with stem diameter greater than 8 cm were randomly selected for sap flow monitoring (eight trees in total). In addition to these eight trees, a fenced site was established on each geological formation, where sap flow sensors were installed on neighbouring pine and cypress trees (four trees in total), with a *P. lentiscus* shrub located on the other side of each of these two tree species (Figure 2 and Figure 3). All 12 trees were equipped with a sap flow sensor working with a Heat Ratio Method (SFM1, ICT International, Armidale, Australia), which, in contrast to the Granier-type thermal dissipation probes, does not require calibration (Fuchs et al. 2017). All sap flow sensors were installed at approximately 30-cm trunk-height in October 2020 and heat pulse velocities were recorded hourly. Sap flow was monitored between 6 October 2020 and 30 June 2022 for the eight trees, and for the four neighbouring trees in the fenced area the monitoring was extended until 31 October 2022. Bark thickness of the monitored trees was measured during sensor installation in October 2020. The tree heights and the canopy cover area of the sap flow trees was derived from the digital surface model (Figure 2). The Leaf Area Index (LAI) was measured with a plant canopy analyser (LAI-2200C, Li-Cor Bioscience, Lincoln, NE, USA) once every 2 months, on all trees with sap flow sensors (Table 2). LAI measurements were made using 90° view cap and skipping the two outer rings (58° and 63°). The rest of the methodology can be found in the protocol in Section 6: Canopy Types; Measuring Isolated Plants in LAI-2200C Instruction Manual (LI-COR Biosciences 2017). The biometrics

TABLE 1 | The number of plants of all tree and shrub species and the number and stem diameter of single stem plants on Athalassa and Nicosia geological formations (February 2020 field survey).

	Number of plants		Number of plants with a single stem		Mean stem diameter (cm)[a]		Standard deviation of stem diameter (cm)	
Plant species	**Athalassa**	**Nicosia**	**Athalassa**	**Nicosia**	**Athalassa**	**Nicosia**	**Athalassa**	**Nicosia**
Pinus brutia	352	494	333	488	10.3	11.1	2.3	2.6
Cupressus sempervirens	102	114	76	84	9.9	10	1.8	1.7
Pistacia lentiscus	168	331	5	11	11.3	14.7	1.1	2.7
Pistacia atlantica	85	113	57	83	9.3	9.4	1.4	1.2
Olea europaea	111	177	14	12	n.a.	8.3	n.a.	0.3
Ceratonia siliqua	14	8	0	2	9.9	10.7	1.8	4.6
Quercus coccifera	14	13	3	1	n.a.	n.a.	n.a.	n.a.
Empty spots	88	158	n.a.	n.a.	n.a.	n.a.	n.a.	n.a.
Total	934	1408	488	681				

[a]Only single stem plants with stem diameter > 8 cm.

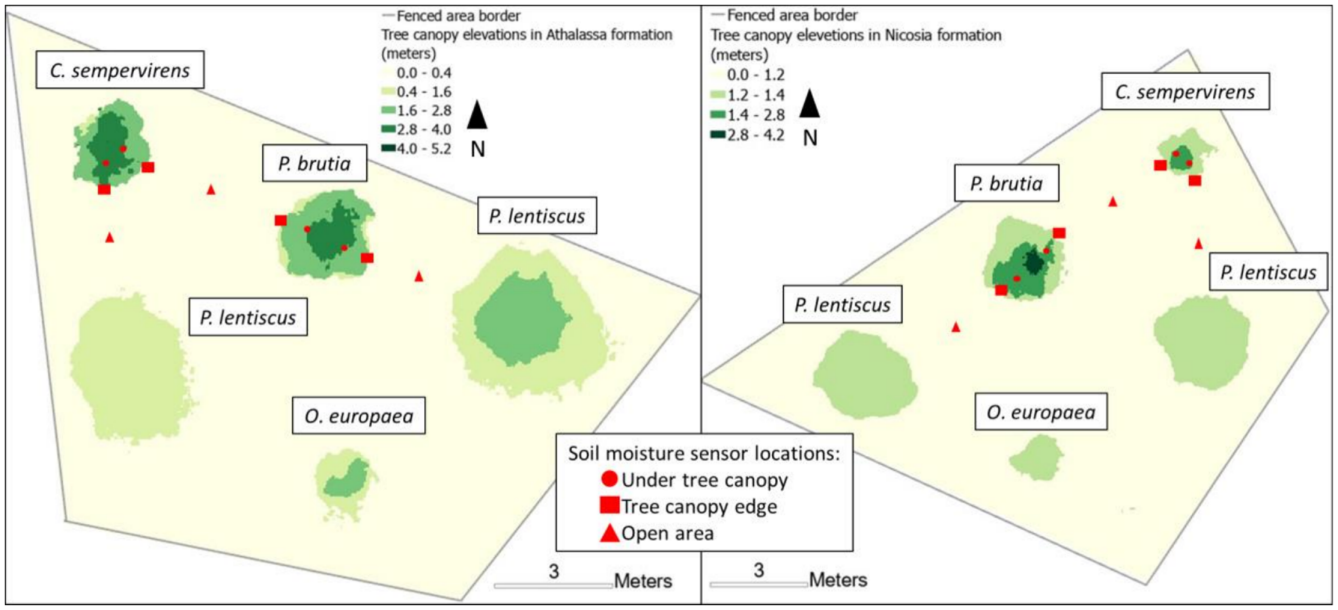

FIGURE 3 | Canopy cover and soil moisture sensor locations for the sap-flow-monitored pine and cypress trees, and adjacent *Pistacia lentiscus* shrubs in the fenced sites on Athalassa (left) and Nicosia (right) formations. The canopy cover is represented in varying shades of green, with darker tones indicating higher elevations.

TABLE 2 | Means and standard deviations (sd) of tree biometrics ($n=6$) and p-values of two-factor ANOVA ($n=3$) between species (pine and cypres) and geologies (Athalassa and Nicosia).

	Pine		Cypress		*p*-value		
	Mean	**sd**	**Mean**	**sd**	**Species**	**Geology**	**Interaction**
Stem diameter (cm)	9.2	1.1	10.3	1.7	0.25	0.18	0.74
Bark thickness (cm)	1.5	N.A.	0.5	N.A.	N.A.	N.A.	N.A.
Sapwood depth (cm)	3.1	0.6	4.7	0.8	**0.01**	0.15	0.79
Tree height (m)	3.5	0.6	3.9	1.0	0.54	0.98	0.94
Canopy cover area (m^2)	7.8	0.9	7.2	2.6	0.65	0.91	0.88
Leaf area index							
May 2021	3.5	1.0	3.0	1.2	0.48	0.19	0.86
May 2022	4.2	1.1	3.8	1.1	0.59	0.07	0.53

Note: p-values <0.05 are given in bold.

of the 12 sap flow trees are summarized in Table 2, the biometrics of individual trees are presented in Table A1.

In October 2020, core samples were extracted from two pine and two cypress trees (random selection, excluding the sap flow sensor installed trees) with an increment borer (5.15 mm diameter) to measure the sapwood depth. Sapwood sampled trees had similar stem diameters (mean for pine was 9 cm and for cypress it was 10 cm) to the sap flow sensor installed trees (Table 2). Intra-species stem diameter variation in the study site was also small (Table 1) compared with natural forests (e.g., Eliades et al., 2019) as all trees were planted at the same time. Indicator dye (methyl orange and methyl blue) was applied to determine the sapwood depth from the difference in colour between the sapwood and the heartwood area. The same increment borer was used for sampling sapwood fresh and dry weight for calculating sapwood density and wood thermal diffusivity based on Marshall (1958). Sapwood samples were collected in April 2022 from six pine and six cypress trees in close proximity to the trees with sap flow sensors, whose sizes (canopy volume and trunk circumference) were the same as those of the trees with the sensors. Mean water content of the sapwood was the same for both pine and cypress (43%). Mean sapwood density was 0.59 g cm^{-3} for pine and 0.55 g cm^{-3} for cypress (p-value = 0.27); mean thermal diffusivity was 0.0027 $cm^2 s^{-1}$ (p-value = 0.23) for both pine and cypress. Heartwood was not observed in any of the core samples.

Zero sap flow baseline was set visually and the sap velocity was calculated according to Burgess et al. (2001) using the Sap flow Tool software (Burgess and Downey 2014). Sap flow was calculated by multiplying the sap velocity (cm h^{-1}) with the corresponding cross-sectional area (cm^2) of the sapwood.

SFM1 sap flow sensors have 35-mm long needles and thermistors are located at 7.5 and at 22.5 mm from the tip of the needles. The sapwood area is divided into concentric annuli delimited by the midpoints between the measurement depths and sap velocities are weighted according to their annulus sizes. Sap velocity in the sapwood area beyond the measurement depth is assumed to linearly reduce towards the centre of the stem. Linear regression relations were developed between the hourly sap flow observations of same tree species on same geology and in the cases of sensor failure; missing data were filled using these relations.

2.2.3 | Physiological Measurements

Twig water potential (Ψ) and leaf conductance (*gs*) were measured on the two pine and two cypress trees in the fenced sites and on four pine and four cypress trees around the fenced sites. Both Ψ and *gs* were measured around mid-day between (10:00 and 13:00 h), which typically represents the period of minimum diurnal twig water potential. Measurements were made on 14 July 2021, 9 September 2021, 10 November 2021 and 5 April 2022. Only *gs* was measured on 27 June 2022. Ψ was measured with a pressure chamber (1505D, PMS Instrument Company, Albany, USA) (one measurement per tree) and *gs* was measured with a leaf porometer (SC-1, METER Group, Munich, Germany) on two sun-facing leaves per tree.

2.2.4 | Meteorological Monitoring

A solar-powered meteorological sensor (ATMOS 41, METER Group, Munich, Germany) was installed at 2-m height in December 2020 in the fenced sites in the Nicosia formation. The station was placed in the spacing between the shrubs and trees to represent the micro-meteorological conditions of the site. The station was located at a distance of 3.5 m from the nearest Cypress tree (3.3 m height) and 5-m from the nearest pine tree (3.6 m height), whereas the other neighbouring species (*P. lentiscus*, *P. atlantica* and *Olea europa*) are less than 2 m high. Precipitation, relative humidity, temperature, incoming radiation, wind speed, wind direction, atmospheric pressure and air vapour pressure were recorded at 5-min time intervals. Data from two other meteorological stations were used to fill gaps in our ATMOS 41 data time series, one was the Athalassa governmental meteorological station located around 1 km from the experimental site, and the other one was from the meteorological sensors of an eddy covariance tower instrumented at a height of 2 m in a neighbouring agricultural field (at 500 m distance). Gaps were filled with data from these stations without any data manipulation due to close proximity of these stations to the study site. Daily reference evapotranspiration was computed with the FAO56 Penman-Monteith equation (Allen et al. 1998).

2.2.5 | Soil Moisture Monitoring

Sixty-six soil moisture sensors (SMT100, Truebner, Germany) with four small battery-powered data-loggers (TrueLog 100, Truebner, Germany) were installed in November 2020 (33 sensors per geological formation) (Figure 3) in linear transects between the neighbouring pine and cypress trees, and in the adjacent *P. lentiscus* shrubs in the two fenced sites. In each fenced site, soil moisture sensors were installed at 11 locations representative of the three canopy cover conditions: (i) under the tree canopy cover (approximately halfway between the trunk and the canopy edge), (ii) at the canopy cover edge and (iii) in the open area without tree canopy cover in the middle between the trees. The sensors were installed at soil depths of 10, 30 and 50 cm. The soil moisture sensor measurement interval was hourly.

2.2.6 | Biomass of Seasonal Vegetation

The biomass of the seasonal vegetation was collected from open areas without tree canopy cover at the end of spring (May 2021 and May 2022) to assess possible differences in the effect of seasonal vegetation on evapotranspiration between years. The sampling and analyses protocol was modified from ICOS Ecosystem protocols for grassland and for forest (Gielen et al. 2017; Op de Beeck et al. 2017). The biomass samples were collected with a $25 \times 25\,cm^2$ quadrat at 40 randomly selected locations in the study site. The centre point for the quadrat was the centre point of the linear distance between trees/shrubs. All aboveground biomass within the quadrat was cut to ground level, put in paper bags and taken to the laboratory. Samples were placed in a drying oven at 65°C until constant weight was achieved, and then the dry biomass was weighted.

2.3 | Analysis

2.3.1 | Tree Sap Flow

Daily mean sap velocities ($m\,day^{-1}$) and sap flows over the sapwood area ($10^{-3}\,m^3\,day^{-1}$) and over the tree canopy area ($mm\,day^{-1}$) of four periods (1 November 2020 to 30 April 2021, 1 May 2021 to 31 October 2021, 1 November 2021 to 30 April 2022, and 1 May 2022 to 30 June 2022) were tested with a two-factor ANOVA for the two species and two geologies without data transformation. Normality was tested with Shapiro–Wilk Test and homogeneity of variances was tested with Levene's Test.

2.3.2 | Plant-Environment Interactions

Partial correlation coefficients were calculated between daily midday values (mean of 10:00 to 13:00 h) of sap flow (mean of 6 trees per species) and each environmental variable, by controlling the effect of all other environmental variables, with the package *ppcor* (Kim 2015) in R 3.2.2. The midday values of the sap flow and environmental variables were also tabulated against the Ψ and *gs* observations.

2.3.3 | Water Balance Calculations and Soil Water Dynamics

Water balances of each of the three canopy cover conditions (under-canopy, edge of canopy and open area) were calculated

with the use of the average soil moisture (SM) per depth from the sensors on either side of the trunk of each tree species ($n = 2$), on each geologic formation. These water balance equations follow a data-driven approach, constrained by observed soil moisture, precipitation and the maximum evaporative demand, calculated from the meteorological observations. Rainfall interception is included in the evapotranspiration. Deviations in soil moisture are compensated by soil water and runoff flows (Q) driven by heterogeneities in the soil profile. The evapotranspiration and soil water flows for a 60-cm soil column representing the three canopy covers were calculated as follows:

$$ET_{p(t)} = MAX\left(P_{(t)} - \Delta SM_{(t)} + Q_{(t-1)}, 0\right) \text{ for } P_{(t-1)} > 0 \text{ and } Q_{(t-1)} > 0 \quad (1a)$$

$$ET_{p(t)} = MAX\left(P_{(t)} - \Delta SM_{(t)}, 0\right) \text{ for } P_{(t)} > 0 \text{ and } Q_{(t-1)} \leq 0 \quad (1b)$$

$$ET_{p(t)} = MAX\left(-\Delta SM_{(t)}, -\Delta SM10_{(t)}, 0\right) \text{ for } P_{(t)} = 0 \text{ and } Q_{(t-1)} \leq 0 \quad (1c)$$

$$ET_{a(t)} = MIN\left(K_{cmax} \times ET_{0(t)}, ET_{p(t)}\right) \quad (2)$$

$$Q_{(t)} = P_{(t)} - \Delta SM_{(t)} - ET_{a(t)} \quad (3)$$

$$K_{cmax} = 1.2 + \left[(0.04 * (u - 2)) - 0.004 * (RH - 45) * \left(\frac{h}{3}\right)^{0.3}\right] \quad (4)$$

where $ET_{p(t)}$ is the potential and $ET_{a(t)}$ is the actual evapotranspiration from the 60-cm soil column on day t; $P_{(t)}$ is the observed precipitation on day t; $SM_{(t)}$ is the total soil water moisture of the 0 to 60-cm soil column, observed with the soil moisture sensors at 10-, 30- and 50-cm depths (each sensor representing 20 cm soil layer thickness) at 0:00 h of day t; ΔSM is computed by subtracting $SM_{(t)}$ from $SM_{(t+1)}$; $Q_{(t)}$ represents the net flow out of the soil water column (positive) or into the soil column (negative), such as surface runoff, drainage and lateral flows, on day t; $SM10_{(t)}$ is the soil moisture of the top 20-cm layer on day t, derived from the 10-cm depth sensors; K_{cmax} is the maximum crop coefficient (Allen et al. 1998); u is the mean value of the average daily wind speed (1.3 m s^{-1}); RH the mean value of the average daily minimum relative humidity (43%); and h is the tree height (3.7 m). The indices t, $t-1$, $t+1$ identify the daily time step.

Equations (1a)–(1c) first calculate ET_p based on the water balance, and Equation (2) then calculates the ET_a based on the atmospheric demand. Equation (1a) represents the case where the water balance on the previous rain day had a net water loss (positive Q). This loss could have been surface runoff, drainage or small rainfall events and preferential flow processes that may not have been captured by the soil moisture sensors, or canopy interception storage that may not have fully evaporated during the day. On the day after the rain day, a net water gain (negative Q) is often observed. This could be because Darcy flows filled more soil pores in the soil profile, while evapotranspiration losses from the soil could also be low because part of the atmospheric demand was used to evaporate the previous day's left-over interception storage. With Equation (1a), this net water gain (negative Q) is filled with the net water balance loss from the previous rain day (positive $Q_{(t-1)}$). For all other cases, ET_p on rain days is calculated from the water balance with Equation (1b); and ET_p on dry days is calculated with Equation (1c). Equation (1c) checks if the soil water loss of the top soil layer is higher than the total water loss in the soil profile. If this is the case, ET_p is set to the soil water loss of the top layer. Here, the assumption is that due to soil evaporation and transpiration from seasonal plants, the soil water head gradient in the upper layer exceeds the gradient between the upper and lower soil layers, while soil water increases in the lower layers could be due to lateral flows or capillary upward flows, as computed in Equation (3).

The area provided for each tree during plantation (i.e., the circular area centring the tree to the half way of the neighbouring tree) is considered tree planting area. To assess how evapotranspiration over the tree planting area (ET_{ap}) and canopy area (ET_{ac}) compare with the observed tree transpiration over these areas, the following equations were used (see Figure 3):

$$ET_{ap} = \frac{A_u}{A_p} * ET_{au} + \frac{A_e}{A_p} * ET_{ae} + \frac{A_o}{A_p} * ET_{ao} \quad (5)$$

$$A_p = A_u + A_e + A_o \quad (6)$$

$$ET_{ac} = \frac{A_u}{A_c} * ET_{au} + \frac{A_e/2}{A_c} * ET_{ae} \quad (7)$$

$$A_c = A_u + \frac{A_e}{2} \quad (8)$$

$$A_u = \Pi r_u^2 \quad (9)$$

$$A_e = \Pi r_e^2 - A_u \quad (10)$$

$$A_o = \Pi r_o^2 - A_u - A_e \quad (11)$$

where ET_{au}, ET_{ae} and ET_{ao} are the evapotranspiration amounts calculated (Equations 1–4) for under, edge and open canopy conditions, respectively; A_p is the circular tree planting area, A_c is the canopy area; A_u, A_e and A_o are area fractions and circular areas representative of under-canopy, edge of canopy and open area canopy cover conditions, respectively; r_u is the average distance between the tree trunk and the mid-point between under canopy and edge of canopy soil moisture sensors, r_e is the average distance between the tree trunk and the length of the mid-point between the under canopy and edge of canopy soil moisture sensors mirrored outwards into the open area and r_o is the average distance between the tree trunk and the open area soil moisture sensor location.

The water use efficiency (WUE) of the seasonal plants were calculated by dividing the biomass of the plants (Section 2.2.6) by ET_{ao}. In both years, the seasonal plants started emerging early December. In the first, dry year plants had completely dried by the end of March 2021. In the wetter 2021–2022 year, plants had dried by the end of April 2022. Total ET_{ao} of these months in which the seasonal plants were active, were used for the WUE of the two seasons.

3 | Results

3.1 | Tree Sap Flows

The two-factor ANOVA of the sap flow variables showed no interaction between species and geology at a statistical significance level of 0.05 (Table 3, individual tree values are presented in Table A2). Similarly, except for the sap velocity during the short May to June 2022 period, the effect of geology was always insignificant (p-value >0.05). This finding is supported by the similar soil texture for both geologies (Section 2.1), the similar average soil moisture during these four periods (Table A3) and the absence of significant differences between the tree biometrics on the two geologies (Table 2).

Over the 20-month observation period, the mean sap flow over the canopy area of cypress trees was more than double that of pine (p-value $=0.02$). The difference in mean sap flows (over the stem area) of the two species was similarly significant. This difference was statistically more significant during warmer months with less rain (49.4 mm for May 2021 to October 2021 and 75.8 mm May 2022 to June 2022), compared to the colder months with more rain (186.7 mm for November 2020 to April 2021 and 269.2 mm for November 2021 to April 2022). Mean sap velocity did not show significant differences between pine and cypress, except for the wet November 2021 to Apr 2022 period, when pine sap velocity was almost two times higher. Considering individual trees, for each species, sap velocity was always lowest for trees with the largest sapwood depths, whereas average sapwood depth was larger for cypress than for pine (Tables A1 and A2).

3.2 | Plant–Environment Interactions

The cypress trees show continuously substantial higher sap flow than pine for the November 2020 to April 2021 period, compared to the same period in the following year, when the difference between species is less obvious (Figure 4, sap flow velocities are presented in Figure A1). The main difference

TABLE 3 | Mean sap velocities and sap flows with standard deviations (sd) per species ($n=6$) and p-values of two-factor ANOVA ($n=3$) between species (pine and cypress) and geologies (Athalassa and Nicosia).

	Pine		Cypress		p-value		
	Mean	**sd**	**Mean**	**sd**	**Species**	**Geology**	**Interaction**
November 2020 to April 2021							
Mean velocity ($m\,day^{-1}$)	1.2	0.4	1.0	0.4	0.45	0.83	0.39
Mean flow ($10^{-3}\,m^3\,day^{-1}$)	4	1	8	4	0.09	0.62	0.72
Total flow (m^3)	0.7	0.2	1.4	0.3			
May 2021 to October 2021							
Mean velocity ($m\,day^{-1}$)	1.1	0.3	1.1	0.4	0.84	0.40	0.22
Mean flow ($10^{-3}\,m^3\,day^{-1}$)	3	1	7	2	**0.00**	0.59	0.22
Total flow (m^3)	0.6	0.2	1.3	0.3			
November 2021 to April 2022							
Mean velocity ($m\,day^{-1}$)	1.5	0.5	0.9	0.4	**0.04**	0.20	0.38
Mean flow ($10^{-3}\,m^3\,day^{-1}$)	4	1	5	2	0.22	0.66	0.10
Total flow (m^3)	0.8	0.2	1.0	0.3			
May 2022 to June 2022							
Mean velocity ($m\,day^{-1}$)	2.0	0.4	1.7	0.6	0.24	**0.03**	0.23
Mean flow ($10^{-3}\,m^3\,day^{-1}$)	6	1	10	3	**0.01**	0.17	0.06
Total flow (m^3)	0.4	0.1	0.6	0.2			
November 2020 to June 2022							
Mean velocity ($m\,day^{-1}$)	1.5	0.4	1.2	0.4	0.18	0.15	0.22
Mean flow ($10^{-3}\,m^3\,day^{-1}$)	4	1	7	2	**0.02**	0.90	0.27
Total flow (m^3)	2.4	0.7	4.3	1.3			
Mean flow over canopy area ($mm\,day^{-1}$)	0.5	0.2	1.1	0.4	**0.02**	0.80	0.43
Total flow over canopy area (mm)	314	103	642	225			

Note: p-values <0.05 are given in bold. Sapwood areas per tree were kept constant for the sap flow calculations throughout the monitoring period. Because the share of the flow per tree is not the same in each season, the ratio between flow and velocity differs by season.

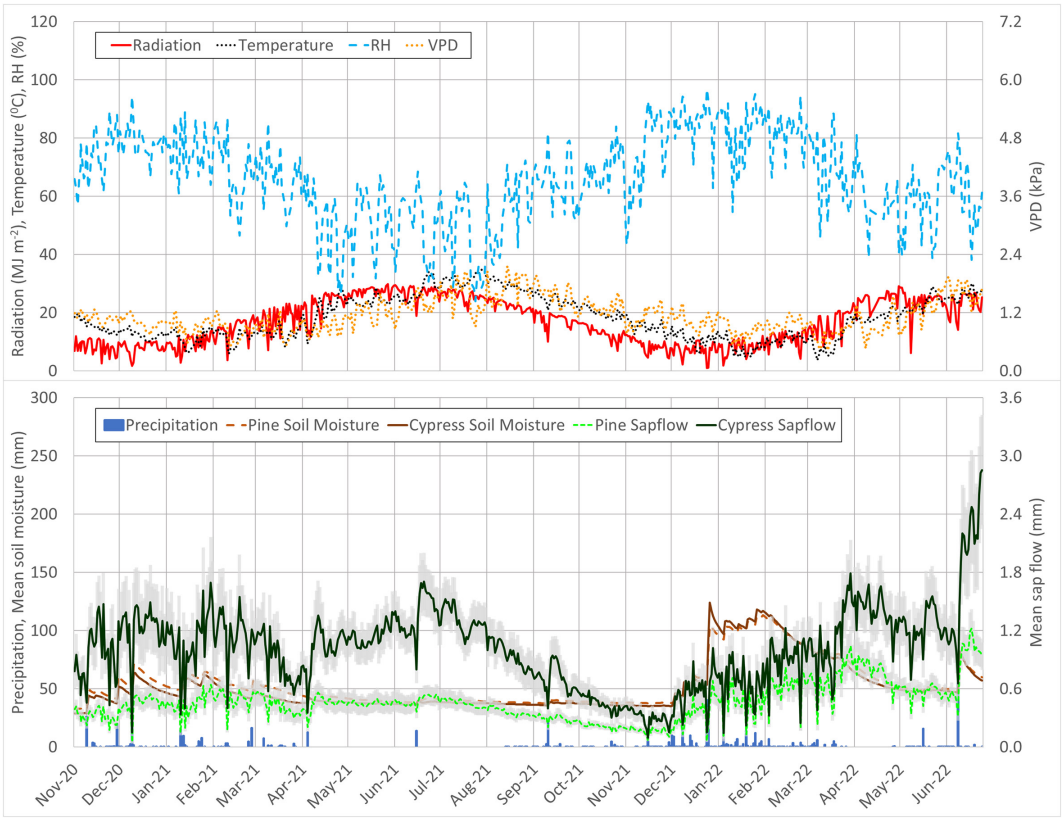

FIGURE 4 | Daily total radiation, mean temperature, relative humidity (*RH*), vapour pressure deficit (*VPD*) (top); daily total precipitation, soil moisture in the 60-cm rootzone (average of 2 trees per species, each with 2 under canopy and 2 edge of canopy locations, all with sensors at 10-, 30-, 50-cm depths), average total daily sap flow over the canopy area, with standard error ($n = 6$ per species), for the November 2020 to June 2022 measurement period.

between these periods is the amount of precipitation. Total precipitation for the drier November 2020 to April 2021 period was 186.7 mm, whereas it was 269.2 mm for the wetter November 2021 to April 2022 period. This is also reflected in the higher soil moisture contents in the wetter year. The observed radiation and air temperature were higher during the drier period than during the wetter period. Average radiation was 13 Mj m^{-2} day^{-1} and temperature was 14°C for the drier period and for the wetter period they were 11 Mj m^{-2} day^{-1} and 12°C, respectively. Interestingly, total sap flow of cypress showed a decrease from the drier to the wetter period (1.4 m^3 vs. 1.0 m^3), whereas total pine sap flow showed an increase (0.7 m^3 vs. 0.8 m^3).

Diurnal sap flow patterns of pine and cypress showed differences over the 20-month observation period. Pine had lower maximum hourly sap flow values than cypress and generally reached its maximum sap flow earlier in the day than cypress. These differences were larger on hotter days with high solar radiation (April to October) than on colder days with low solar radiation (November to March). On 13–15 April 2021 (Figure 5a), as example of cloudless spring and summer days, solar radiation reached its daily maximum at 12:00 noon, while pine reached its maximum sap flow at 10:00 and cypress at 13:00 (3 h difference). On winter days with relatively stable solar radiation, such as 3, 4 and 7 January 2022 (Figure 5b), solar radiation reached its daily maximum between 12:00 and 14:00. Pine reached its maximum sap flow at 11:00 and cypress at 12:00 on 3 January, pine at 12:00 and cypress at 13:00 on the 4 January and both trees at 13:00 on the 7 January having no more than 1 h difference. These figures also illustrate the effect of environmental conditions on changes in daily sap flows. Under the low soil moisture conditions in April 2021 (Figure 5a), pine sap flow was lower than cypress sap flow, but was less impacted by the atmospheric conditions of the 12.4-mm rainfall event (low *Rad*, low *T*, high *RH* and low *VPD*). Under the higher soil moisture conditions in December 2021 (Figure 5b), the effect of the changes in atmospheric conditions related to a 2-day 71-mm rainfall event was similar for pine and for cypress.

All partial correlation coefficients between sap flow and environmental variables were higher for pine than for cypress (Table 4 and scatter plots in Figure A3). For both species, correlations were higher for soil moisture than for radiation. However, only the partial correlation between pine sap flow and soil moisture was higher than 0.5.

The stomatal conductance (*gs*) of pine and cypress showed a similar response to environmental conditions (Table 5). However, pine had a wider range of *gs* values and a narrower range of Ψ values than cypress. The *gs* and sap flow of both species were low under the low *SM* in July and September 2021 and high under the higher *SM* in April and June 2022. Under the higher *SM* conditions, the *gs* of both species showed a small decrease, in response to the higher *Rad*, *T* and *VPD* of June 2022 versus April 2022, while the sap flow increased.

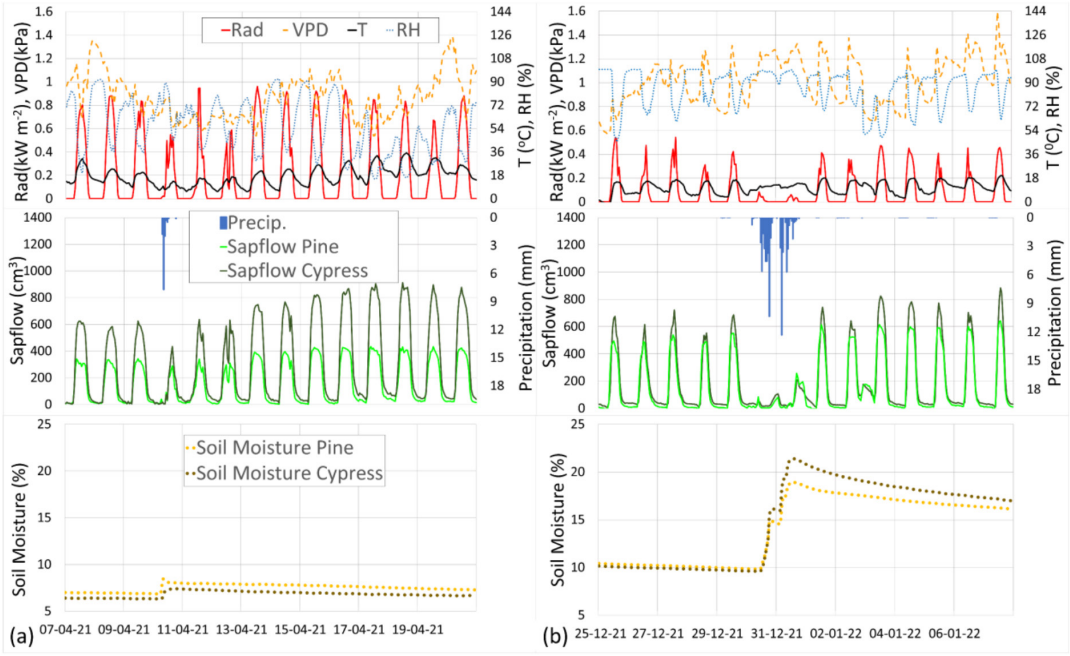

FIGURE 5 | Diurnal patterns of hourly tree sap flow ($n = 6$ per tree species) of pine and cypress and environmental variables (*Rad*: radiation; *T*: air temperature; *RH*: relative humidity; *VPD*: vapour pressure deficit; *SM*: soil moisture (average of 2 trees per species, with 2 under canopy and 2 edge of canopy locations and 10-, 30-, 50-cm depths; $n = 24$ for each species) during 7 to 20 April 2021 (a) and 25 December 2021 to 7 January 2022 (b).

TABLE 4 | Partial correlation coefficients between daily midday values (means between 10:00 and 13:00 h) of sap flow (means of 6 trees per species) and environmental variables.

	Sap flow pine	Sap flow cypress
Radiation	0.17*	0.04
Temperature	−0.36*	−0.23*
Relative humidity	−0.35*	−0.32*
Vapour pressure deficit	0.29*	0.17*
Soil moisture	0.66*	0.31*

*p-values < 0.05.

This sap flow increase was higher for cypress than for pine. Remarkably, the Ψ of cypress showed a strong response to *SM*, increasing from an average of −3.1 MPA for the first three measurement dates to −1.3 MPa at the higher *SM* in April 2022. The *gs* was higher in November 2021 than in September 2021, while *SM* remained low and *Rad*, *T*, *VPD* and also sap flow decreased. For pine, the higher *gs* was also reflected by a lower Ψ.

3.3 | Water Balances and Soil Water Dynamics

Total precipitation for the 1 November 2020 to 31 October 2021 period was 236.2 mm (dry year) and for the 1 November 2021 to 31 October 2022 period it was 475.5 mm (wet year). In the cumulative water balance component plots, daily precipitation events can be seen as abrupt increases, whereas daily tree transpiration [i.e., sap flow over tree canopy area (T_c) and over tree planting area (T_p)] showed gradual increase after these precipitation events (Figure 6). The cumulative transpiration over the canopy area (T_c) of cypress started to exceed the cumulative evapotranspiration over the canopy area (ET_{ac}) in June in the dry year and in July in the wet year. In the dry year, cypress T_c also exceeded the rainfall over the canopy area. In the dry year, T_c was 42% of ET_{ac} for pine and 127% for cypress. In the wet year, pine T_c was 37% of the ET_{ac} and cypress T_c was 112% of the ET_{ac}. Over the full planting area (28.3 m^2), transpiration (T_p) constituted still a small fraction of the evapotranspiration (ET_{ap}): 19% for pine and 34% for cypress in the dry year and 16% (pine) and 32% (cypress) in the wet year. However, during the summer months of July and August 2021, daily ET_{ac} and ET_{ap} dropped to almost zero, while tree transpirations (T_c and T_p) remained relatively constant (Figure A2). During these months, the T_p of both species was more than 100% of the ET_{ap} (127% for pine and 279% for cypress). Over the 1 November 2020 to 30 June 2022 period, the T_c means of the two pine trees (296 mm) and two cypress trees (566 mm) in the fenced areas used in this water balance analysis were similar as the mean of all six monitored pine (314 mm) and cypress trees (642 mm).

Location-specific evapotranspiration values showed variations (Figure 6). Cumulative ET_{ao} was the highest, ET_{au} was the lowest and ET_{ae} was in between, for both species and both years. The computed losses (Q) of under-canopy locations were almost two times higher than those of the open areas. The two-year under canopy Q for pine was slightly higher than cypress (15-mm difference) (not presented). Even though the cumulative ET_{au} over the 2 years for pine and cypress are nearly similar, the average soil moisture for cypress (41 and 63 mm in dry and wet year, respectively) was lower than the average soil moisture for pine (48 and 66 mm in dry and

TABLE 5 | Means and standard deviations (sd) of midday stomatal conductance (*gs*), twig water potential (Ψ) and sap flow ($n = 6$ per species) and midday means of radiation (*Rad*), air temperature (*T*), relative humidity (*RH*), vapour pressure deficit (*VPD*) and soil moisture (*SM*) (means of values between 10:00 and 13:00 h).

	gs (mmol m^{-2} s^{-1})				Ψ (MPa)				Sap flow (cm^{-3} h^{-1})				Environmental variables				
	Pine		Cypress		Pine		Cypress		Pine		Cypress		*Rad*	*T*	*RH*	*VPD*	*SM*
	Mean	sd	Mean	sd	Mean	sd	Mean	sd	Mean	sd	Mean	sd	Wm^{-2}	°C	%	kPa	%
14-07-2021	65.1	27.0	62.9	15.8	−0.9	0.6	−3.2	0.4	309	88.9	825	204.2	872	38	28	1.4	6.7
09-09-2021	54.5	11.0	59.7[a]	18.3[a]	−1.0	0.6	−3.0	1.2	206	57.6	457	104.3	623	32	43	1.6	6.2
10-11-2021	117.0	21.6	86.8	17.2	−1.5	0.7	−3.1	0.6	181	53.7	285	49.3	342	21	48	1.0	6.3
05-04-2022	119.2	31.2	89.8	19.8	−1.4	0.3	−1.3	0.1	649	208.3	901	266.5	633	22	54	1.1	11.8
27-06-2022	113.9	17.6	87.7	14.5	N.A.	N.A.	N.A.	N.A.	677	156.4	1135	499.7	758	31	38	1.3	11.1

[a]Mean and sd of five measurements, after removal of a 265 mmol m^{-2} s^{-1} outlier.

wet year, respectively). These differences are illustrated in Figure 7, which shows the mean and standard errors of the hourly soil moisture values of the three locations and three depths for pine and cypress, for the 2-day 73.7-mm rainfall event during 30 December 2021 to 2 January 2022. Soil moisture values under the canopy at the 10- and 30-cm soil depths showed higher standard errors after rainfall for pine than for cypress, which also resulted in higher *Q* for pine than for cypress during this 4-day period (25 mm vs. 5 mm).

The ET_{ao} midway between two trees was similar between couples of different species (see sensor locations in Figure 3 and Figure 8). In the dry year ET_{ao} was 221 mm between *P. brutia* and *C. sempervirens* trees, 228 mm between *P. lentiscus* and *P. brutia* and 223 mm between *P. lentistus* and *C. sempervirens*. In the wet year, these numbers were 367, 335 and 329 mm, respectively. The aboveground biomass of the seasonal plants in the open areas was 0.54 kg m^{-2} in May 2021 and 0.48 kg m^{-2} in May 2022, showing no significant difference between years (p-value = 0.52). The WUE of seasonal plants was 3.9 kg m^{-3} in the dry year and 2.7 kg m^{-3} in the wet year.

4 | Discussion

Sap velocities between *C. sempervirens* and *P. brutia* did not show significant differences (p-value > 0.05) for the majority of the 20-month observation period, except for the wet November 2021–April 2022 period (p-value = 0.04) when pine sap velocity was 67% higher than cypress sap velocity. However, *C. sempervirens* trees had significantly larger sapwood depths than *P. brutia* (p-value = 0.01), which resulted in higher sap flow for *C. sempervirens* for the full observation period. Stem diameter, tree height, canopy cover area and LAI showed no statistically significant differences (p-value > 0.05) between species (Table 2). The higher sap flow for *C. sempervirens*, as observed in the present study, align with findings from other studies involving *C. sempervirens* and *P. halepensis* in a 50-year-old mixed forest in Israel with an annual rainfall of approximately 500 mm (Lapidot et al. 2019; Rog et al. 2021). Lapidot et al. (2019) found higher transpiration rates for *C. sempervirens* (around 2 mmol H_2O m^{-2} s^{-1}) than for *P. halepensis* (around 1 mmol H_2O m^{-2} s^{-1}) during midday and afternoon measurements with a gas exchange system for 2 days in March, under natural conditions. They attributed the higher transpiration of *C. sempervirens* to its higher leave temperature, which could be the result of denser foliage and darker leave colour than that of *P. halepensis*. It should be noted that sap velocity within the sapwood can have radial and azimuthal variability (Cohen et al. 2008). For the sap flow computations a linear reduction of sap velocity beyond the measurement depth towards the centre of the sapwood was assumed (see Section 2.2.2). Eliades et al. (2019) found, with Heat Field Deformation measurements, that sap velocity of *P. brutia* trees showed a linear decrease with sapwood depth. Cohen et al. (2008) reported similar radial sap velocity change (second order polynomial regression with leading coefficients of 0.0002) for 15- to 19-year-old *P. halepensis* and *C. sempervirens* trees. Therefore, even though the average radius of the sapwood of the cypress trees was 4.7 cm and that of the pine trees was 3.1 cm, no major differences in the uncertainties of the computed sap flow of the two species were assumed. With respect to azimuthal

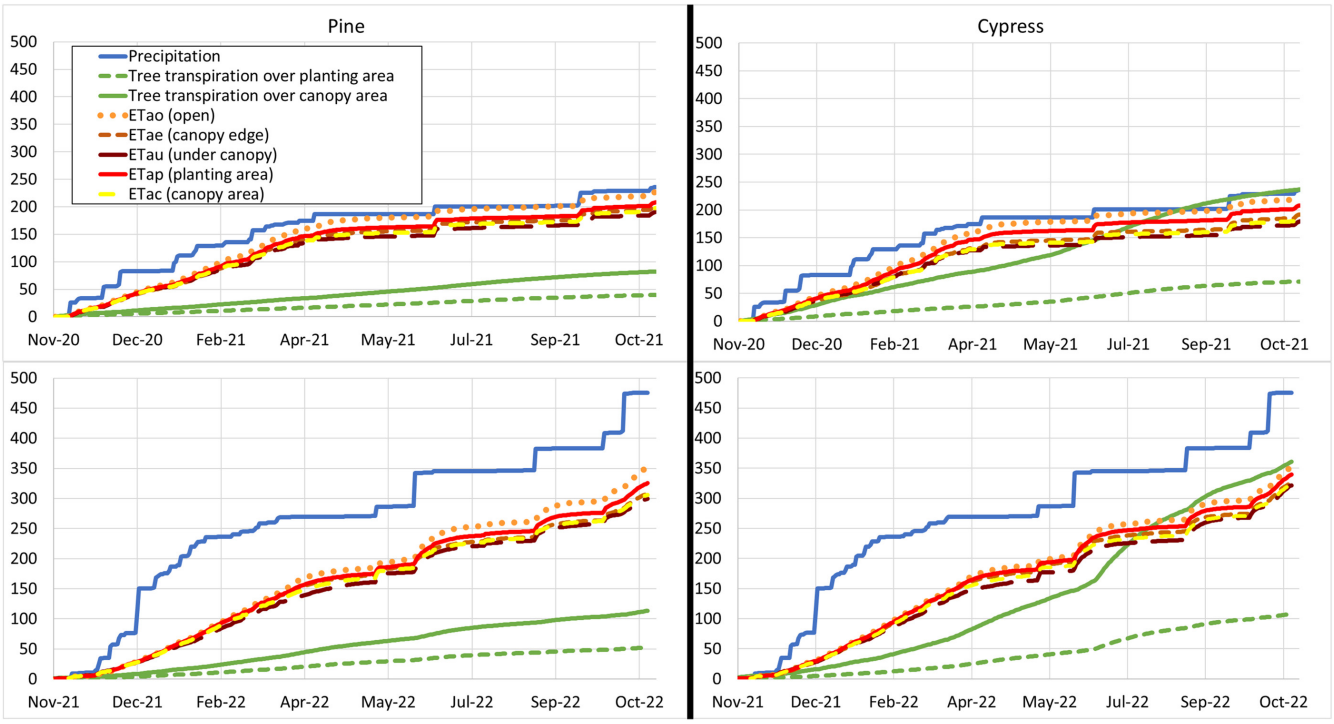

FIGURE 6 | Cumulative tree transpiration and evapotranspiration over canopy and planting areas, evapotranspiration of the three canopy locations and precipitation between 1 November 2020 and 31 October 2021 (top) and between 1 November 2021 and 31 October 2022 (bottom) for pine (left) and cypress (right), average of two trees of each species on two geologic formations.

variations, Eliades et al. (2018) found that sap flow of *P. brutia* observed with north facing sensors was 1 to 4% lower than that if south facing sensors. This effect was ignored in the current study. Further research with heat field deformation sensors and heat ratio method sensors installed at different azimuths can help quantifying radial and azimuthal differences in sap velocities (e.g., Reyes-Acosta and Lubczynski 2014).

Some of the measured sap flow could be used for the internal tree water storage and would not immediately become transpiration, as observed by Preisler et al. (2022) in a 50-year-old, semi-arid *P. halepensis* forest in Israel. They measured soil moisture, transpiration and sap flow continuously, accompanied by periodical measurements of stem and twig water potential and water content of sapwood and twigs, using a flux tower, gas exchange chambers and sap flow sensors. They found that internal tree water storage can contribute 23% to 45% of the total daily transpiration during the dry season. The lower stomatal conductance values and range of *C. sempervirens*, compared with *P. brutia*, may have resulted in higher use of internal water storage for transpiration, which could be part of the higher sap flow increase of *C. sempervirens* after summer rain, as observed in the present study. However, no difference between the water content of the sapwood of *P. brutia* and *C. sempervirens* was observed at the time of sapwood sample collection in April 2022, indicating similar sapwood water storages.

P. brutia sap flow correlations with environmental variables were higher than *C. sempervirens* sap flow correlations, especially with soil moisture and radiation. *P. brutia* seems to react to soil moisture increase by increasing its sap flow even during relatively dark winter days. This could be because of the more open canopy structure of *P. brutia* compared with *C. sempervirens*. Schiller et al. (2004) found that midday sap flow velocity of C. *var. horizontalis* trees was greater than that of C. *var. pyramidalis* trees partly because of their more open canopy structure, which determines the radiation regime within the canopy as well as the airflow through it.

The values of *gs* for *P. halepensis* and *C. sempervirens* reported in Rog et al. (2021) were similar as the values in the present study ($< 100\,\text{mmol}\,\text{m}^{-2}\,\text{s}^{-1}$ on all 4 measurement days for cypress and 2 days for pine). Similarly, these authors observed that *P. halepensis* showed substantial increases in *gs* in June–August while *C. sempervirens* showed little change. Rog et al. (2021) also observed lower pre-dawn Ψ values for *C. sempervirens* (−4.6 MPa) than for *P. halepensis* (−2.3 MPa) in September although these values were lower than the midday values observed in the present study in September (−3.0 MPa for *C. sempervirens* and −1.0 MPa for *P. brutia*). Although differences between *P. halepensis* and *C. sempervirens* observed by Rog et al. (2021) were similar as those between *P. brutia* and *C. sempervirens* observed in the present study, differences between these two pine species (*P. halepensis* and *P. brutia*) have also been reported in the literature. Houminer et al. (2022) found earlier reduction of *gs* and transpiration by *P. halepensis* in response to drought stress, compared to *P. brutia*, in greenhouse experiments with 18-month old rooted cuttings.

More variable *gs* and relatively stable Ψ for *P. brutia* compared to *C. sempervirens* indicates that *P. brutia* reduces its stomatal conductance to keep a near constant minimum leaf water potential, which limits leaf transpiration and thereby helps to minimize water loss. This same type of behaviour was also

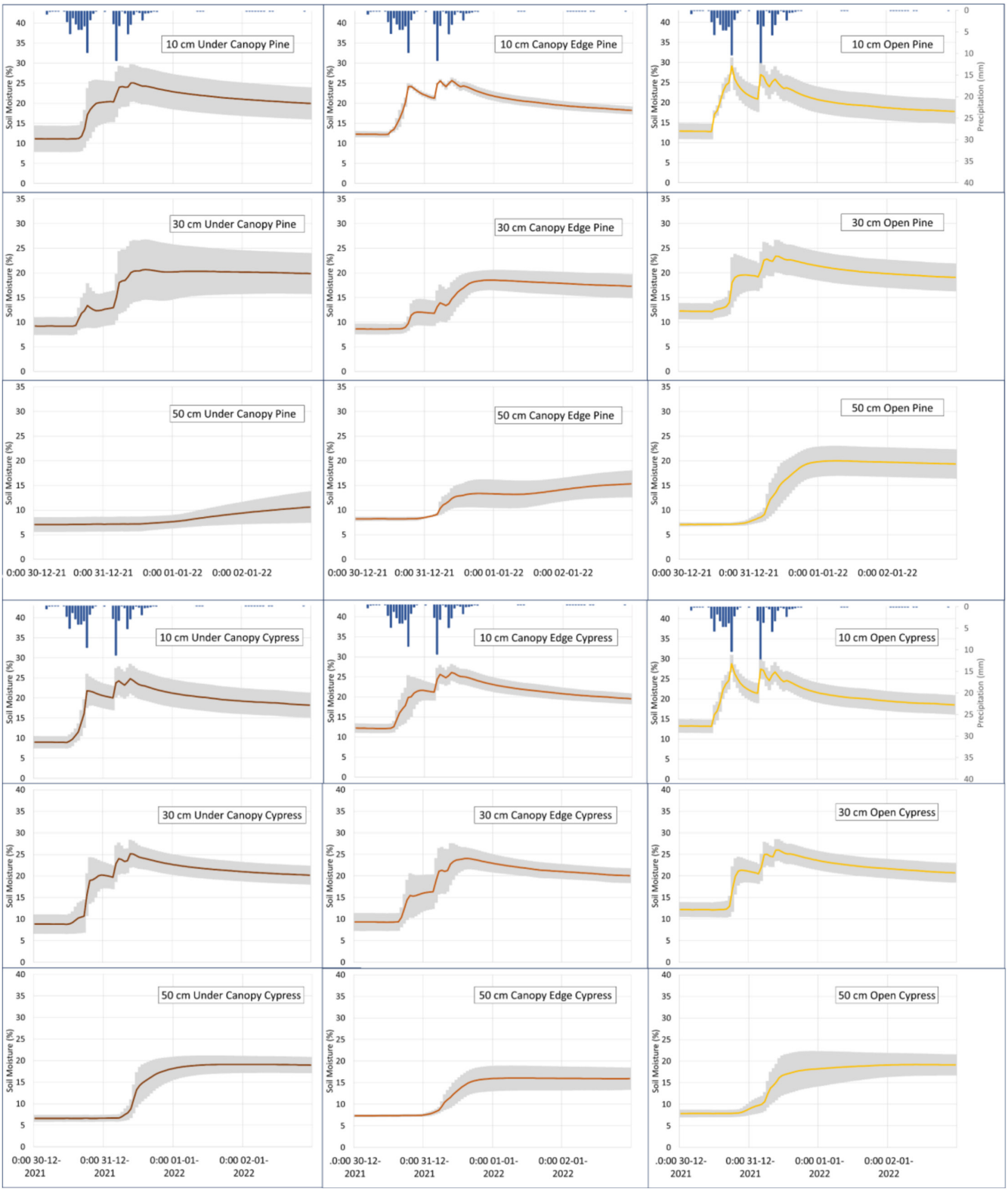

FIGURE 7 | Mean and stand errors (grey bars) of hourly soil moisture values (%) during 30 December 2021 to 2 January 2022 in open ($n = 4$), canopy edge ($n = 4$) and under canopy ($n = 4$) locations for pine (a) and cypress (b).

observed for 18-month-old *P. halepensis* trees in a controlled experiment by Klein et al. (2011). In contrast, *C. sempervirens* was found to maintain leaf transpiration by keeping its stomata open during the day, thereby ensuring continuous water uptake. The contrasting hydraulic behaviour of *P. halepensis* and *C. sempervirens* trees was also observed in another greenhouse experiments on 18-month-old trees by Froux et al. (2005). Whereas such behaviour has been referred to as isohydric (*P. brutia*) and anisohydric (*C. sempervirens*), Hochberg et al. (2018) pointed out that plants can shift from anisohydric to isohydric behaviour

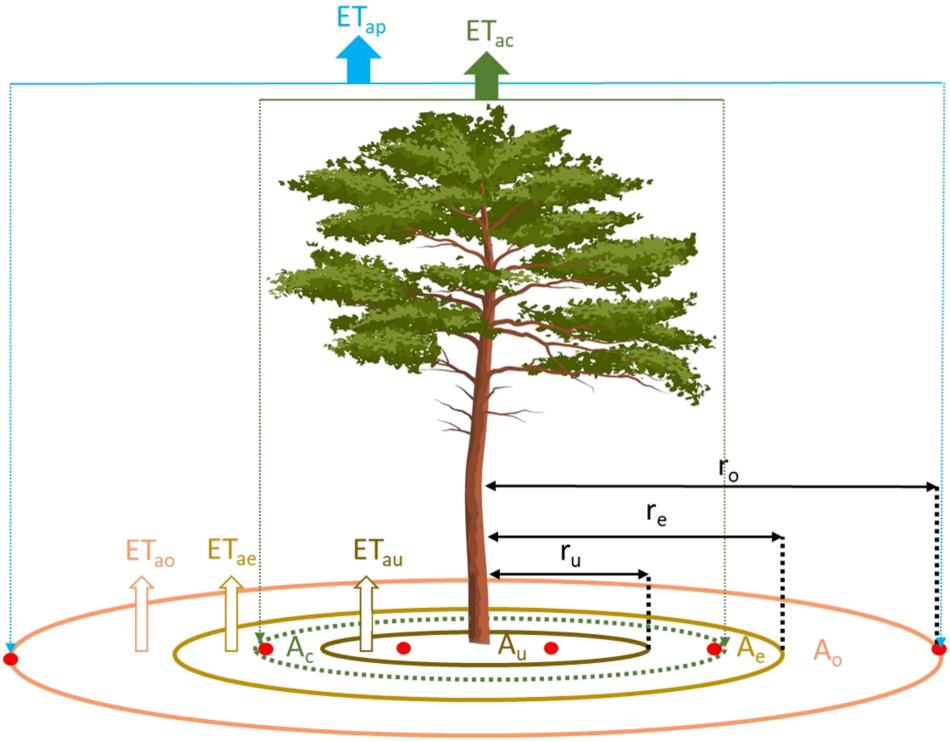

FIGURE 8 | Soil moisture sensor locations (red dots) and different ET_a's with their respective areas (ET_{au}: under canopy, ET_{ae}: edge canopy, ET_{ao}: open area, ET_{ac}: canopy area and ET_{ap}: planting area evapotranspirations).

depending on soil water contents and that these classifications are affected by the duration and frequency of observations. This was also the case for the present study as sap flow (hourly observations for 20 months) showed more pronounced differences between *P. brutia* and *C. sempervirens* during dry months than wet months.

It was observed in the present study that T_c of *C. sempervirens* was more than 100% of the precipitation over the canopy cover area and more than 100% of the ET_{ac}. This indicates that the *C. sempervirens* trees abstract water, with its roots, beyond the canopy area and deeper than 60-cm. Moreover, during the summer months of July and August 2021, the T_p of both species was more than 100% of the ET_{ap} (127% for *P. brutia* and 279% for *C. sempervirens*), as derived from the 66 soil moisture sensors. This indicates that both trees can take up water beyond the 60-cm soil depth. Similar observations were made by Rog et al. (2021), who sampled soil cores and identified tree species based on DNA in a mixed forest stand of *P. halepensis*, *C. sempervirens*, *Ceratonia Siliqua*, *Quercus calliprinos*, and *P. lentiscus*. Their analyses showed that, regardless of the proximity to any tree species, sampled soil layers were dominated by only two tree species, namely *P. lentiscus* and *C. sempervirens*. The roots of *P. halepensis* accounted for only 14%–23% of the roots growing around *P. halepensis* trees. They also found that root growth of *C. sempervirens* was mostly horizontal, whereas root growth of *P. halepensis* was both horizontal and vertical. The quicker increase of *C. sempervirens* sap flow after a relatively small rainfall event and the more stable *P. brutia* sap flow observed in the present study can also be indications of more horizontal *C. sempervirens* roots and more vertical *P. brutia* roots. Location-specific evapotranspiration values showed differences in the present study. The lower ET_{au} compared with ET_{ao} could be due to preferential flows under the tree canopies caused by the tree branches and stems, which concentrate rainwater at specific points, and by the tree roots, which channel soil water below the 60-cm soil depth. These theories were supported by the hourly soil moisture values. The greatest standard errors were observed for the sensors under the canopy, compared with the sensors at the canopy edge and open areas. These standard errors were higher for pine than for cypress, which can be attributed to the physiological differences between these two species. For example, the measured LAI values for pine were slightly higher than for cypress, though differences were not significant (p-value > 0.05) and the surface texture of pine tree bark is rougher than the surface texture of cypress tree bark. These differences can affect the rainwater throughfall and stemflow (Eliades et al. 2022), which increases the variability of the soil moisture under the canopy.

The mean seasonal plant biomass in the dry year was not significantly different from the biomass of the wet year, indicating that the transpiration of the seasonal plants was similar in the 2 years. However, plant growth benefitted from the higher temperature and radiation in the dry year (average 14°C and 13 Mj m^{-2} day^{-1} during the November to April period) compared to the wet year (12°C and 11 Mj m^{-2} day^{-1}). This effect is also seen in the higher sap flow for cypress in the dry year, relative to the wet year, but not for pine. More root growth during drier years compared to wet years can also be the reason for higher sap flow rates for cypress (Rog et al. 2024). The high ET_{ao} in the dry year, averaging 95% of precipitation, indicates that the seasonal plants in the open area could compete with the trees. In the wet year, average ET_{ao} was 72% of the precipitation, with the remainder flowing below the 60-cm soil depth or laterally as surface runoff and subsurface flows for use by the trees. Navarro et al. (2010) found small differences in annual understory

biomass productivity of a thinned *P. halepensis* forest, with similar tree density as this study (30 m^2 per tree), during 3 years when rainfall ranged between 268 and 370 mm $year^{-1}$, but the understory productivity dropped sharply during a dry year with 204 mm rain.

Planting mixed tree species to reduce competition and use water effectively has been a topic of several research papers (Bello et al. 2019; Fruleux et al. 2020; De Cáceres et al. 2021; Magh et al. 2020; Rog et al. 2021; Zhang et al. 2019), as there is a growing demand from forest managers to identify practices that reduce the effects of projected water scarcity in the coming decades. In the current study, differences in sap flow, *gs* and Ψ showed that *P. brutia* and *C. sempervirens* have different water use strategies and these differences were more pronounced during the dry year, supporting the research hypothesis. However, the evapotranspiration of the open areas did not show substantial differences between couples of different species (*P. brutia*, *C. sempervirens* and *P. lentiscus*). This indicates that there may not have been competition for soil water between these 12- and 13-year old trees and shrubs.

5 | Conclusions

It can be concluded from 20 months of hourly sap flow monitoring that *C. sempervirens* trees transpire significantly more than the *P. brutia* trees. Sap flow of *C. sempervirens* can be more than double that of *P. brutia* during the summer months. The importance of soil moisture for these trees in this semi-arid environment is highlighted, as both increased their sap flow rates when soil moisture increased after rain. However, partial correlation coefficients between tree sap flow and soil moisture were much higher for *P. brutia* than for *C. sempervirens* trees, whereas partial correlations with radiation were low for both. Measurements of *gs* and Ψ indicated that *P. brutia* regulates its stomatal conductance to keep a near constant minimum twig water potential, which limits leaf transpiration and thereby helps to minimize water loss. This contrasts with *C. sempervirens* whose twig water potential decreased with decreasing soil moisture, thereby maintaining transpiration. Soil water balance calculations showed that transpiration of *P. brutia* trees was around 40% of the evapotranspiration from the 60-cm soil depth of its canopy area, both for a dry and a wet year, whereas it exceeded 100% for *C. sempervirens* in both years. However, both species extracted water below the 60-cm soil depth and beyond the canopy cover area during the summer months of dry as well as wet years. Despite differences in tree transpiration, under-canopy ET_a was the lowest, canopy-edge ET_a was in between and open-area ET_a was the highest, for both species and both years. The lower ET_a from the 60-cm soil depth under the canopy, compared to ET_a in the open area, could be due to preferential flow losses caused by tree branches, stems and roots. Although *P. brutia* and *C. sempervirens* trees are both coniferous species with needle and scale-like leaves and are considered to be drought tolerant, it can be concluded that they have different strategies to cope with water stress. Long-term continuous monitoring programmes can improve the understanding of the effects of the highly variable and changing climate on tree and shrub species in such harsh semi-arid ecosystems. Further research could also investigate the carbon budgets (above and below ground) and water use efficiencies of *P. brutia* and *C. sempervirens* trees.

Acknowledgements

We would like to thank the Ministry of Agriculture, Rural Development and Environment of Republic of Cyprus, specifically the Department of Forests for sharing knowledge and hosting the research site and the Department of Meteorology for providing meteorological data. We thank Melpo Siakou and Giouli Venetsanou for their help with the fieldwork. We are grateful to the three reviewers for their constructive suggestions and comments.

Data Availability Statement

The data that support the findings of this study are available from the corresponding author upon reasonable request.

References

Al-Hawija, B. N., V. Wagner, and I. Hensen. 2014. "Genetic Comparison Between Natural and Planted Populations of *P. brutia* and *C. sempervirens* in Syria." *Turkish Journal of Agriculture and Forestry* 38, no. 2: 267–280. https://doi.org/10.3906/tar-1211-24.

Allen, R. G., L. S. Pereira, D. Raes, M. Smith. 1998. *FAO Irrigation and Drainage Paper No. 56 Crop Evapotranspiration*. Food and Agriculture Organization of the United Nations. Volume 300.

Bello, J., P. Vallet, T. Perot, et al. 2019. "How Do Mixing Tree Species and Stand Density Affect Seasonal Radial Growth During Drought Events?" *Forest Ecology and Management* 432: 436–445. https://doi.org/10.1016/j.foreco.2018.09.044.

Boydak, M. 2004. "Silvicultural Characteristics and Natural Regeneration of *P. brutia* ten.: A Review." *Plant Ecology* 171, no. 1/2: 153–163. https://doi.org/10.1023/B:VEGE.0000029373.54545.d2.

Brofas, G., G. Karetsos, C. Tsagari, and P. Dimopoulos. 2006. "The Natural Environment of *C. sempervirens* in Greece as a Basis for Its Use in the Mediterranean Region." *Land Degradation and Development* 17, no. 6: 645–659. https://doi.org/10.1002/ldr.750.

Burgess, S. S. O., M. A. Adams, N. C. Turner, et al. 2001. "An Improved Heat Pulse Method to Measure Low and Reverse Rates of Sap Flow in Woody Plants." *Tree Physiology* 21, no. 9: 589–598. https://doi.org/10.1093/treephys/21.9.589.

Burgess, S. S. O., and A. Downey. 2014. *SFM1 Sap Flow Meter Manual*. ICT international Pty Ltd.

Caudullo, G., and D. De Rigo. 2016. "*Cupressus sempervirens* in Europe: Distribution, Habitat, Usage and Threats." In *European Atlas of Forest Tree Species*, edited by J. San-Miguel-Ayanz, D. de Rigo, G. Caudullo, T. Houston Durrant, and A. Mauri, e01afb4+. Publ. Off. EU, Luxembourg.

Chapman, M., W. S. Walker, M. Farina, et al. 2020. "Large Climate Mitigation Potential From Adding Trees to Agricultural Lands." *Global Change Biology* 26, no. 8: 4357–4365. https://doi.org/10.1111/gcb.15121.

Cohen, Y., S. Cohen, T. Cantuarias-Aviles, and G. Schiller. 2008. "Variations in the Radial Gradient of Sap Velocity in Trunks of Forest and Fruit Trees." *Plant and Soil* 305, no. 1/2: 49–59. https://doi.org/10.1007/s11104-007-9351-0.

Cyprus Geological Survey Department. 1995. "Geological Map of Cyprus." https://geoportal-gsd.moa.gov.cy/portal/apps/experiencebuilder/experience/?id=a18a7b0a0c494ef8abc21be965a07308&page=Home.

De Cáceres, M., M. Mencuccini, N. Martin-StPaul, et al. 2021. "Unravelling the Effect of Species Mixing on Water Use and Drought Stress in Mediterranean Forests: A Modelling Approach." *Agricultural*

and Forest Meteorology 296: 108233, N.PAG. https://doi.org/10.1016/j.agrformet.2020.108233.

Eliades, M., A. Bruggeman, H. Djuma, A. Christou, K. Rovanias, and M. W. Lubczynski. 2022. "Testing Three Rainfall Interception Models and Different Parameterization Methods With Data From an Open Mediterranean Pine Forest." *Agricultural and Forest Meteorology* 313: 108755. https://doi.org/10.1016/j.agrformet.2021.108755.

Eliades, M., A. Bruggeman, H. Djuma, M. W. Lubczynski, A. Christou, and C. Camera. 2018. "The Water Balance Components of Mediterranean Pine Trees on a Steep Mountain Slope During Two Hydrologically Contrasting Years." *Journal of Hydrology* 562: 712–724. https://doi.org/10.1016/j.jhydrol.2018.05.048.

Ellison, D., C. E. Morris, B. Locatelli, et al. 2017. "Trees, Forests and Water: Cool Insights for a Hot World." *Global Environmental Change Part A: Human & Policy Dimensions* 43: 51–61. https://doi.org/10.1016/j.gloenvcha.2017.01.002.

EUFORGEN. 2025. "European Forest Genetic Resources Programme." Accessed April 15, 2025. https://www.euforgen.org/species.

Fan, Y., G. Miguez-Macho, E. G. Jobbágy, R. B. Jackson, and C. Otero-Casal. 2017. "Hydrologic Regulation of Plant Rooting Depth." *Proceedings of the National Academy of Sciences of the United States of America* 114, no. 40: 10,572–10,577. https://doi.org/10.1073/pnas.1712381114.

Froux, F., E. Dreyer, M. Ducrey, and R. Huc. 2005. "Vulnerability to Embolism Differs in Roots and Shoots and Among Three Mediterranean Conifers: Consequences for Stomatal Regulation of Water Loss?" *Trees-Structure and Function* 19, no. 2: 137–144. https://doi.org/10.1007/s00468-004-0372-5.

Fruleux, A., M.-B. Bogeat-Triboulot, C. Collet, and D. Bonal. 2020. "Lack of Effect of Admixture Proportion and Tree Density on Water Acquisition Depth for European Beech (*Fagus sylvatica* L.) and Sycamore Maple (*Acer pseudoplatanus* L.)." *Annals of Forest Science* 77, no. 2: 36. https://doi.org/10.1007/s13595-020-00937-1.

Fuchs, S., C. Leuschner, R. Link, H. Coners, and B. Schuldt. 2017. "Calibration and Comparison of Thermal Dissipation, Heat Ratio and Heat Field Deformation Sap Flow Probes for Diffuse-Porous Trees." *Agricultural and Forest Meteorology* 244–245: 151–161. https://doi.org/10.1016/j.agrformet.2017.04.003.

Gielen, B., M. Op de Beeck, F. Michilsens, and D. Papale. 2017. "ICOS Ecosystem Instructions for Ancillary Vegetation Measurements in Forest (Version 20,200,330)." *ICOS Ecosystem Thematic Centre*. https://doi.org/10.18160/4ajs-z4r9.

Hochberg, U., F. E. Rockwell, N. M. Holbrook, and H. Cochard. 2018. "Iso/Anisohydry: A Plant–Environment Interaction Rather Than a Simple Hydraulic Trait." *Trends in Plant Science* 23, no. 2: 112–120. https://doi.org/10.1016/j.tplants.2017.11.002.

Houminer, N., Y. Osem, R. David-Schwartz, J. Riov, and M. Moshelion. 2022. "Comparison of Morphological and Physiological Traits Between *P. brutia*, *P. halepensis*, and Their Vigorous F1 Hybrids." *Forests* 13, no. 9: 1477. https://doi.org/10.3390/f13091477.

IPCC. 2023. In *Sections. In: Climate Change 2023: Synthesis Report. Contribution of Working Groups I, II and III to the Sixth Assessment Report of the Intergovernmental Panel on Climate Change*, edited by Core Writing Team, H. Lee, and J. Romero, 35–115. IPCC. https://doi.org/10.59327/IPCC/AR6-9789291691647.

Jasechko, S., Z. D. Sharp, J. J. Gibson, S. J. Birks, Y. Yi, and P. J. Fawcett. 2013. "Terrestrial Water Fluxes Dominated by Transpiration." *Nature* 496, no. 7445: 347–350. https://doi.org/10.1038/nature11983.

Kim, S. 2015. "Ppcor: An R Package for a Fast Calculation to Semi-Partial Correlation Coefficients." *Communications for Statistical Applications and Methods* 22, no. 6: 665–674. https://doi.org/10.5351/CSAM.2015.22.6.665.

Klein, T., D. Yakir, and S. Cohen. 2011. "Hydraulic Adjustments Underlying Drought Resistance of *P. halepensis*." *Tree Physiology* 31, no. 6: 637–648. https://doi.org/10.1093/treephys/tpr047.

Kostopoulou, P., O. Dini-Papanastasi, and K. Radoglou. 2010. "Density and Substrate Effects on Morphological and Physiological Parameters of Plant Stock Material of Four Forest Species Grown in Mini-Plugs." *Scandinavian Journal of Forest Research* 25: 10–17. https://doi.org/10.1080/02827581.2010.485826.

Lapidot, O., T. Ignat, R. Rud, I. Rog, V. Alchanatis, and T. Klein. 2019. "Use of Thermal Imaging to Detect Evaporative Cooling in Coniferous and Broadleaved Tree Species of the Mediterranean Maquis." *Agricultural and Forest Meteorology* 271: 285–294. https://doi.org/10.1016/j.agrformet.2019.02.014.

LI-COR Biosciences. 2017. *LAI-2200C Plant Canopy Analyser Instruction Manual (Revision 5)*. LI-COR Biosciences.

Magh, R.-K., C. Eiferle, T. Burzlaff, H. Rennenberg, M. Dannenmann, and M. Dubbert. 2020. "Competition for Water Rather Than Facilitation in Mixed Beech-Fir Forests After Drying-Wetting Cycle." *Journal of Hydrology* 587: 124944. https://doi.org/10.1016/j.jhydrol.2020.124944.

Marshall, D. C. 1958. "Measurement of Sap Flow in Conifers by Heat Transport." *Plant Physiology* 33, no. 6: 385–396.

Navarro, F. B., M. N. Jiménez, E. Gallego, L. Terrón, M. A. Ripoll, and E. M. Cañadas. 2010. "Effects of Different Intensities of Overstory Thinning on Tree Growth and Understory Plant-Species Productivity in a Semi-Arid *Phalepensis* Mill. afforestation." *Forest Systems* 19, no. 3: 410–417. https://doi.org/10.5424/fs/2010193-8858.

Obanawa, H., S. Sakanoue, and T. Yagi 2019. "Evaluating the Applicability of RTK-UAV for Field Management." In *IGARSS 2019–2019 IEEE International Geoscience and Remote Sensing Symposium, Geoscience and Remote Sensing Symposium, IGARSS 2019–2019 IEEE International*, 9090–9092. https://doi.org/10.1109/IGARSS.2019.8897895.

Op de Beeck, M., S. Sabbatini, and D. Papale. 2017. "ICOS Ecosystem Instructions for Ancillary Vegetation Measurements in Grasslands (Version 20,200,316)." *ICOS Ecosystem Thematic Centre*. https://doi.org/10.18160/daaa-x1ng.

Preisler, Y., I. Oz, F. Tatarinov, et al. 2022. "The Importance of Tree Internal Water Storage Under Drought Conditions." *Tree Physiology* 42, no. 4: 771–783. https://doi.org/10.1093/treephys/tpab144.

Reyes-Acosta, J. L., and M. W. Lubczynski. 2014. "Optimization of Dry-Season Sap Flow Measurements in an Oak Semi-Arid Open Woodland in Spain." *Ecohydrology* 7, no. 2: 258–277. https://doi.org/10.1002/eco.1339.

Rog, I., H. Fox, T. Klein, B. Hilman, D. Yalin, and R. Qubaja. 2024. "Increased Belowground Tree Carbon Allocation in a Mature Mixed Forest in a Dry Versus a Wet Year." *Global Change Biology* 30, no. 2: e17172-n/a. https://doi.org/10.1111/gcb.17172.

Rog, I., C. Tague, G. Jakoby, et al. 2021. "Interspecific Soil Water Partitioning as a Driver of Increased Productivity in a Diverse Mixed Mediterranean Forest." *Journal of Geophysical Research: Biogeosciences* 126: e2021JG006382. https://doi.org/10.1029/2021JG006382.

Rundel, P. W. 2019. "A Neogene Heritage: Conifer Distributions and Endemism in Mediterranean-Climate Ecosystems." *Frontiers in Ecology and Evolution* 7: SEP. https://doi.org/10.3389/fevo.2019.00364.

Schiller, G., Y. Moshe, and E. D. Ungar. 2004. "Transpiration of *Cupressus sempervirens* L. as Influenced by Canopy Structure." *Israel Journal of Plant Sciences* 52, no. 1: 9–19. https://doi.org/10.1560/TCGF-4UX6-YXCP-UXCP.

Schlesinger, W. H., and S. Jasechko. 2014. "Transpiration in the Global Water Cycle." *Agricultural and Forest Meteorology* 189–190: 115–117. https://doi.org/10.1016/j.agrformet.2014.01.011.

Sevik, H., and M. Cetin. 2015. "Effects of Water Stress on Seed Germination for Select Landscape Plants." *Polish Journal of Environmental Studies* 24, no. 2: 689–693. https://doi.org/10.15244/pjoes/30119.

Vico, G., S. Manzoni, S. E. Thompson, et al. 2015. "Climatic, Ecophysiological, and Phenological Controls on Plant Ecohydrological Strategies in Seasonally Dry Ecosystems." *Ecohydrology* 8, no. 4: 660–681. https://doi.org/10.1002/eco.1533.

Zhang, X., Y. Wang, Y. Wang, S. Zhang, and X. Zhao. 2019. "Effects of Social Position and Competition on Tree Transpiration of a Natural Mixed Forest in Chongqing, China." *Trees* 33: 719–732. https://doi.org/10.1007/s00468-019-01811-y.

Zittis, G., M. Almazroui, P. Alpert, et al. 2022. "Climate Change and Weather Extremes in the Eastern Mediterranean and Middle East." *Reviews of Geophysics* 60, no. 3: e2021RG000762. https://doi.org/10.1029/2021RG000762.

Scarascia-Mugnozza, G., H. Oswald, P. Piussi, and K. Radoglou. 2000. "Forests of the Mediterranean Region: Gaps in Knowledge and Research Needs." *Forest Ecology and Management* 132, no. 1: 97–109. https://doi.org/10.1016/s0378-1127(00)00383-2.

Appendix

TABLE A1 | Biometrics of individual trees with sap flow sensors per geological formation [Athalassa (Ath.) and Nicosia (Nic.)].

	Pine 1	Pine 2	Pine 3	Pine 4	Pine 5	Pine 6	Cyp. 1	Cyp. 2	Cyp. 3	Cyp. 4	Cyp. 5	Cyp. 6
Geo. formation	Ath.	Ath.	Ath.	Nic.	Nic.	Nic.	Ath.	Ath.	Ath.	Nic.	Nic.	Nic.
Stem diameter (cm)	8.0	8.3	9.9	11.1	8.6	9.5	8.3	10.8	9.5	10.2	9.5	13.7
Bark thickness (cm)	1.5	1.5	1.5	1.5	1.5	1.5	0.5	0.5	0.5	0.5	0.5	0.5
Sapwood depth (cm)	2.5	2.6	3.4	4.1	2.8	3.3	3.6	4.9	4.3	4.6	4.3	6.3
Tree height (m)	3.8	2.4	4.3	3.6	3.7	3.1	4	5	2.5	3.3	3	5.4
Canopy cov. Area (m^2)	7.1	7.3	9.6	7.5	8.3	7.2	6.8	6.1	8.6	5.7	3.8	12.1

TABLE A2 | Individual sap velocity and sap flow values of pine (P) and cypress (C).

	P1	P2	P3	P4	P5	P6	C1	C2	C3	C4	C5	C6
November 2020–April 2021												
Mean velocity ($m\,day^{-1}$)	0.97	1.62	0.86	0.85	1.34	1.76	0.77	1.80	0.96	1.00	0.73	0.98
Mean flow*10^{-3} ($m^3\,day^{-1}$)	2	3	3	4	3	6	3	14	6	7	4	12
Total flow (m^3)	0.34	0.62	0.56	0.81	0.60	1.09	0.57	2.45	1.01	1.20	0.77	2.20
May 2021–October 2021												
Mean velocity ($m\,day^{-1}$)	1.14	1.47	0.64	0.76	1.30	1.49	1.95	1.05	1.01	0.69	1.05	0.73
Mean flow*10^{-3} ($m^3\,day^{-1}$)	2	3	2	4	3	5	8	8	6	5	6	9
Total flow (m^3)	0.41	0.57	0.42	0.74	0.59	0.94	1.46	1.46	1.08	0.85	1.12	1.68
November 2021–April 2022												
Mean velocity ($m\,day^{-1}$)	1.88	1.75	0.99	0.78	1.49	1.99	1.48	1.19	0.76	0.63	0.63	0.45
Mean flow*10^{-3} ($m^3\,day^{-1}$)	4	4	4	4	4	7	6	9	4	4	4	6
Total flow (m^3)	0.67	0.67	0.65	0.75	0.67	1.23	1.09	1.63	0.80	0.75	0.66	1.01
May 2022–June 2022												
Mean velocity ($m\,day^{-1}$)	2.15	2.45	1.98	1.15	1.94	2.38	2.76	2.14	1.71	1.13	1.45	0.93
Mean flow*10^{-3} ($m^3\,day^{-1}$)	4	5	7	6	5	8	11	16	10	8	7	9
Total flow (m^3)	0.26	0.31	0.43	0.37	0.28	0.49	0.68	0.96	0.58	0.46	0.47	0.63
Total November 2020–June 2022												
Mean flow*10^{-3} ($m^3\,day^{-1}$)	3	4	3	4	4	6	6	11	6	5	5	9
Total flow (m^3)	1.68	2.19	2.08	2.67	2.14	3.76	3.80	6.53	3.48	3.32	2.98	5.42
Mean flow over canopy area ($mm\,day^{-1}$)	0.39	0.49	0.35	0.58	0.42	0.85	0.92	1.74	0.66	0.94	1.31	0.74

TABLE A3 | Average soil moisture values (%) per canopy cover condition ($n = 12$ per condition, 4 sensors per 10-, 30-, 50-cm soil depth) for pine and cypress.

	Under canopy pine	Canopy edge pine	Open area pine	Under canopy cypress	Canopy edge cypress	Open area cypress
November 2020 to April 2021	9	8	9	7	8	9
May 2021 to October 2021	7	6	6	6	6	6
November 2021 to April 2022	12	12	12	12	12	12
May 2022 to June 2022	10	9	8	9	9	8

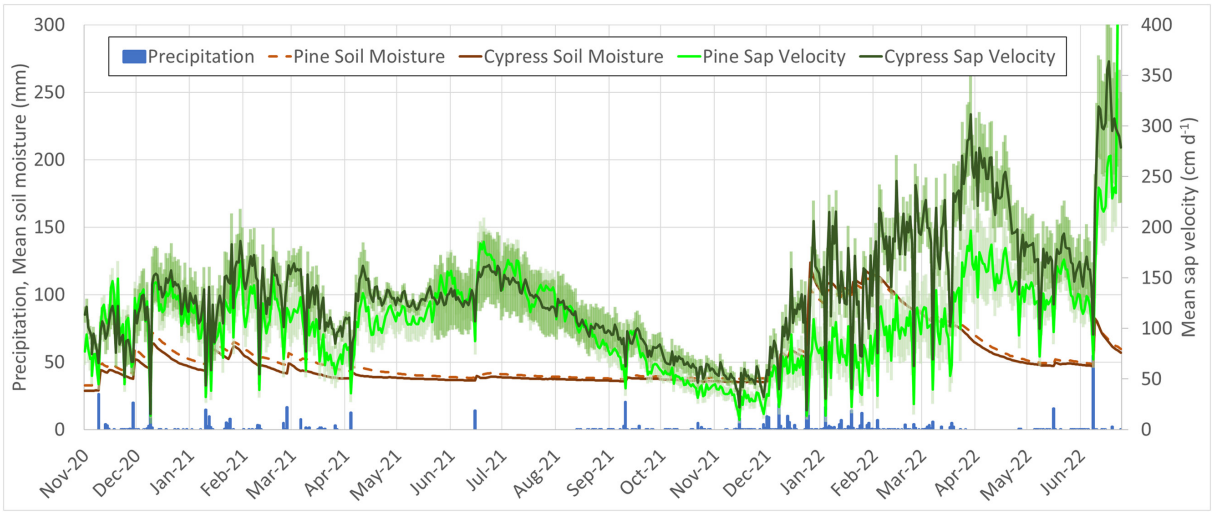

FIGURE A1 | Average daily sap velocity, with standard error ($n = 6$ per species), for the November 2020 to June 2022 measurement period.

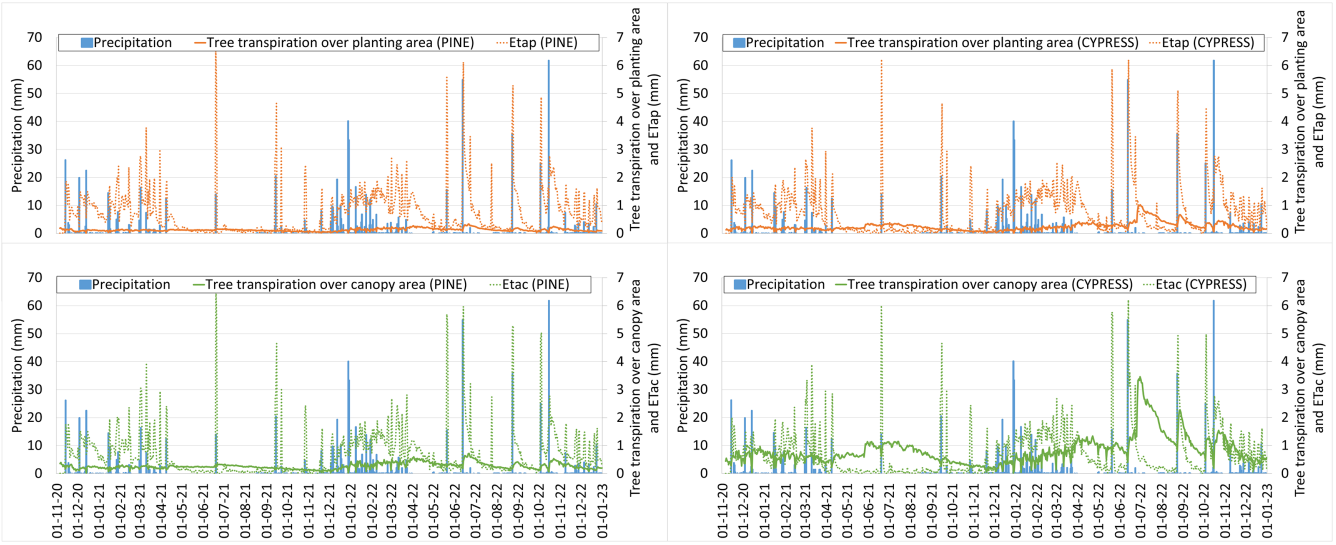

FIGURE A2 | Daily tree transpiration over planting area with ET_{ap} and tree transpiration over canopy area with ET_{ac} for pine and cypress.

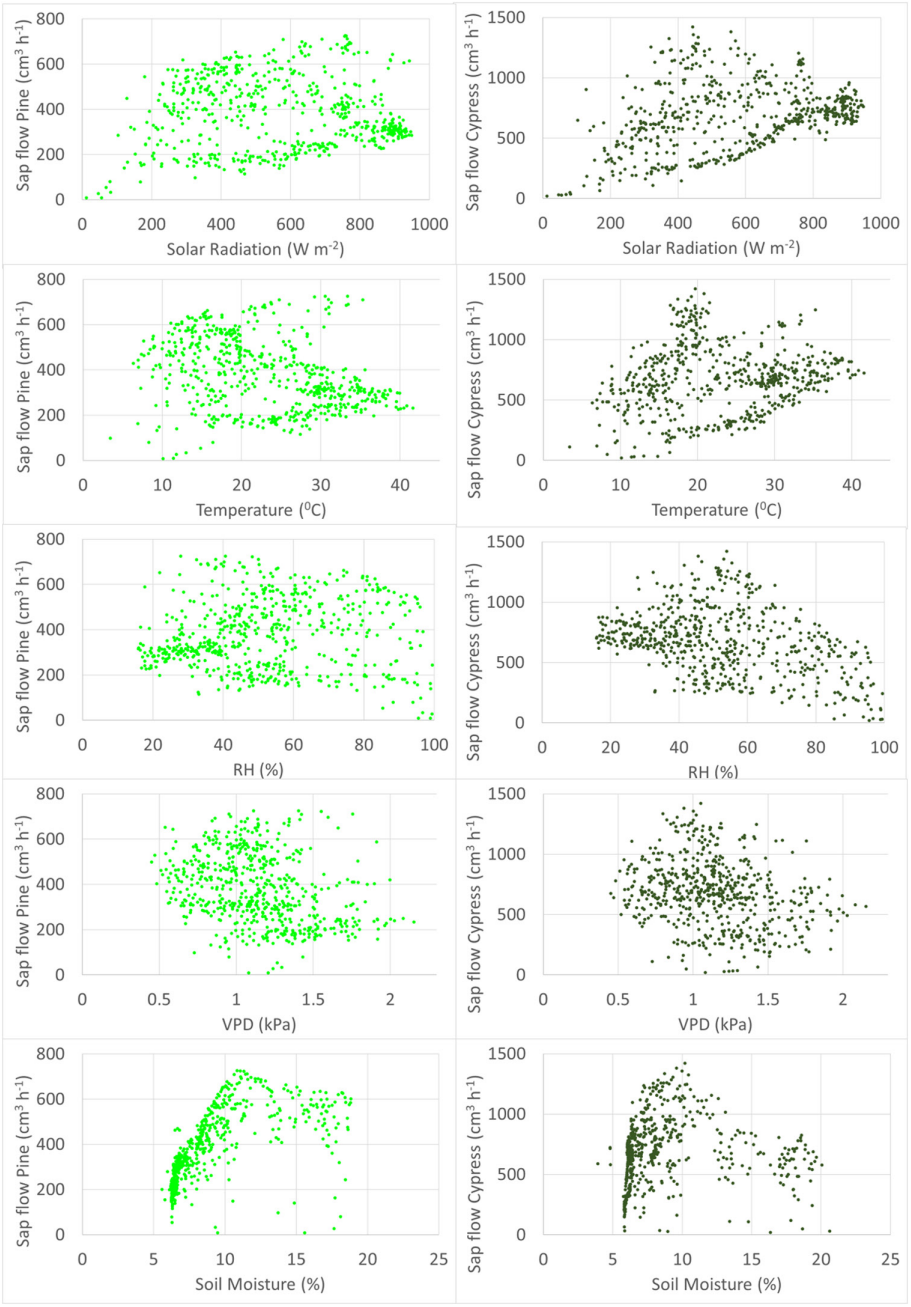

FIGURE A3 | Scattered plots between tree sap flow and environmental parameters.